One-pot facile synthesis of PEGylated Au nanoparticles in an aqueous media

Sevket Tolga Camli [a], Fatih Buyukserin [b], Cafer T. Yavuz [c], Mustafa Selman Yavuz [d,e,∗]

[a] Nanomedicine and Advanced Technologies Research Center, Gazi University, Ankara 06830, Turkey
[b] Department of Biomedical Engineering, TOBB University Eco. & Technol., Ankara 06560, Turkey
[c] Graduate School of EEWS, KAIST, Daejeon 305 701, Republic of Korea
[d] Department of Metallurgical and Materials Engineering, Selcuk University, Konya 42075, Turkey
[e] Advanced Technology Research and Application Center, Selcuk University, Konya 42075, Turkey

ABSTRACT

We describe a facile protocol for the synthesis of PEGylated Au nanoparticles by simply mixing aqueous solutions of $HAuCl_4$ and oligo(ethylene glycol) ethyl ether methacrylate. This method was applied to generate uniform multiply-twinned Au nanostructures of ~ 21 nm in diameter with high yields. Our proposed mechanism indicates that the generation of primary alcohol intermediates from the nucleophilic addition reaction of water (nucleophile) with Au^{III}–vinyl complex is responsible for the reduction of gold ions. This protocol was also used to synthesize Ag nanoparticles and small aggregates of Pd nanoparticles. Due to the exclusion of sophisticated synthesis of PEG containing stabilizers, additional surfactants, or reducing agents, this approach provides a remarkably simple, versatile, and environmentally benign protocol to prepare PEGylated noble-metal nanocrystals. A comparative BSA adsorption study proved the lack of non-specific binding, a common obstacle in designing biocompatible nanoparticles.

© 2012 Elsevier B.V. All rights reserved.

1. Introduction

Among the noble-metal nanoparticles, gold (Au) nanocrystals offer tunable localized surface plasmon resonance (LSPR) [1–3], superior versatility for surface modification [4], excellent chemical stability [5,6], and when properly coated, seamless biocompatibility [7]. The latter, especially, enabled a wide range of biological applications including drug delivery [8,9], DNA sequence detection [10], imaging [11], labeling [12], cancer diagnosis [13], photo-thermal cancer therapy [14,15], and immunosensors [16].

Historically, Au nanoparticles were first reported in 1856 by Michael Faraday who reduced $AuCl_4^-$ ions with phosphorous in aqueous media [17,18]. Since then, various routes based on reduction of Au^{III} salts have been developed. For instance, Turkevich et al. in 1951 formed Au nanoparticles in aqueous solution by reducing $AuCl_4^-$ with sodium citrate, which serves as a reducing agent as well as a stabilizer [19]. In 1994, Brust and coworkers developed a milestone protocol to synthesize Au colloids with relatively narrow size distribution [20]. In their method, Au nanoparticles were obtained in aqueous solution by reducing $AuCl_4^-$ ions with strong reducing agent, sodium borohydrate, in the presence of dodecanethiols (stabilizer) and tetraoctylammonium bromide (a phase transfer agent). Since the Au nanoparticles can be easily generated by simply reducing Au salts, various other reducing agents including amines [21–24], ammonia boranes [25], hydrazine [26], polymers [27,28], and alcohols [29,30] with different capping ligands have been successfully used for the synthesis of Au nanocrystals. None of these methods, however, offer the ultimate, facile, "green" synthesis. Ideally, the sole use of a gold precursor and a biocompatible as well as protein adsorption resistant agent serving as both the reductant and stabilizing agent is desired.

Poly(ethylene glycol) (PEG), a nanoparticle surface modifier, has been widely employed in biological applications as it provides biocompatible and relatively non-toxic platforms that are remarkably resistant to non-specific protein adsorption causing prolonged *in vivo* circulation times in the blood [31–39]. Various methods have been studied to covalently attach PEG onto the surface of Au nanoparticle. Two different approaches are commonly used to

---

generate PEGylated Au nanoparticles (PEG-AuNPs). First one involves the exchange of milder binding surfactants (e.g. citrate ions) on the pre-synthesized Au nanoparticles with PEG-containing strong binding reagents (e.g. thiols and disulfides) [40,41]. For instance, Niidome et al. generated PEGylated Au nanorods by mixing pre-synthesized PEG-SH with the CTAB-coated Au nanorod solution [42]. The other method is to use specially designed and synthesized PEG containing polymeric structures (e.g. block-copolymers, dendrimers) directly in the Au nanoparticle reaction solution as a stabilizer [43–46]. Scrimin and coworkers prepared PEG-AuNPs from the reduction of Au^{III} salts with sodium borohydrate in the presence of pre-synthesized PEG attached octylthiols (stabilizer) [47]. Almost all of these procedures require detailed molecular architecture for PEG modification in order to properly establish Au-PEG nanoparticles. Therefore, a simple and versatile method for the synthesis of PEG-AuNPs is long sought for.

Here, we report a remarkably convenient, one-pot, and green protocol to prepare PEG-AuNPs using an inexpensive and commercially available PEG oligomer, oligo(ethylene glycol) ethyl ether methacrylate (also named "poly(ethylene glycol) ethyl ether methacrylate") (PEGEEM) as both the reductant and stabilizer. The lack of reducing agents and the lengthy multi-step polymer modification procedures make our method an attractive alternative to build PEG-AuNPs. We also demonstrate that other noble metals, such as Ag and Pd, can be made effectively using the same aqueous PEGEEM solution. In addition, the antifouling property of the as-made nanoparticles was demonstrated by protein adsorption studies.

2. Experimental

2.1. Materials

Methyl methacrylate (MMA) was purchased from Merck (Germany) and used as received. Bovine serum albumin (BSA, Fraction V), oligo(ethylene glycol) ethyl ether methacrylate (also named "poly(ethylene glycol) ethyl ether methacrylate" by for instance Aldrich) (PEGEEM), hydrogen tetrachloroaurate (III) hydrate ($HAuCl_4$), silver nitrate ($AgNO_3$) and sodium tetra-chloropalladate (II) (Na_2PdCl_4) were obtained from Aldrich and used as received. Distilled water (Sartorius) was used to prepare all aqueous solutions.

2.2. Synthesis of Au nanoparticles using PEGEEM

In a typical reaction, 51.8 mM aqueous PEGEEM (16 ml) was added to a 25 ml vial equipped with a teflon-coated magnetic stir bar. The vial was inserted to a pre-heated oil bath and stirred for 7 min at 95 °C. Then, 18 μl of aqueous $HAuCl_4$ solution was rapidly added to the vial with a pipette, and the concentration of the $HAuCl_4$ in the reaction solution is 0.057 mM. The reaction mixture was stirred for another 15 min. The product was then collected by centrifugation, and washed twice with water to remove excess PEGEEM and byproducts. Finally, the precipitate was re-dispersed in water for further characterization.

2.3. Synthesis of Pd and Ag nanoparticles using PEGEEM

The procedure to prepare Pd and Ag nanoparticles is essentially the same as the synthesis of Au nanoparticles described above. Pd and Ag nanoparticles were prepared with aqueous 0.172 mM Na_2PdCl_4 and 0.057 mM $AgNO_3$ solutions as the precursors to the corresponding metals. The concentration of PEGEEM used in both reactions is also kept 51.8 mM.

2.4. Synthesis of Au nanoparticles using MMA

The procedure to prepare Au nanoparticles by using MMA is the same as the synthesis of Au nanoparticles using PEGEEM. Au nanoparticles were prepared by adding 0.173 mM $HAuCl_4$ solution to a 25 ml vial containing 156 mM MMA aqueous solution at 95 °C.

2.5. Synthesis of Au nanoparticles using sodium citrate

Citrate-stabilized Au nanospheres were synthesized according to the literature report [51]. In a typical synthesis, 0.27 mM aqueous $HAuCl_4$ (19 ml) was heated to 95 °C. 1 ml of 0.5 wt % sodium citrate was added at once. The color of the solution was turned to pink red within 5 min. TEM micrographs revealed that the nanospheres had an average diameter of 21 nm.

2.6. Non-specific BSA adsorption experiments

PEGEEM and citrate-stabilized Au nanoparticles having an average diameter of 21 nm were used in the non-specific BSA adsorption studies. Various amounts of BSA were dissolved in 0.01 M acetate buffers at pH 5.0. For the equilibrium adsorption experiments, the precipitated nanoparticles were re-dispersed in BSA solutions and then the particle solutions were stirred at 25 °C for 2 h at a rate of 200 rpm. The adsorption equilibrium was established within 30 min as preliminary experiments indicated. After 2 h incubation, the Au nanoparticles were centrifuged and then separated from the adsorption medium. The equilibrium BSA adsorption capacities of the nanoparticles were determined by measuring the initial and final concentrations of BSA adsorption medium through UV absorption at 280 nm.

2.7. Characterization

For SEM and TEM characterization, a drop of the nanoparticle suspension (in water) was placed on a piece of silicon substrate (for SEM) or carbon-coated copper grid (Ted Pella, for TEM), and dried under ambient conditions. SEM images were obtained from FEI Quanta 200 FEG scanning electron microscope. TEM images were recorded with FEI Tecnai G2 Spirit transmission electron microscope operating at 120 kV. UV absorption spectra were taken from Thermo Scientific Biomate 3 Spectrophotometer. Energy-dispersive X-ray (EDX) spectrum was taken from Apollo XL SDD (Edax-Ametek Inc.) detectors integrated to SEM.

3. Results and discussion

PEGylated Au nanocrystals with an average diameter of 21 nm were effectively synthesized from aqueous solutions of $HAuCl_4$ and PEGEEM where PEGEEM serves as the reductant and stabilizer (Fig. 1). A typical synthesis proceeds with the rapid addition of aqueous $HAuCl_4$ solution (0.057 mM) to a clear solution of 51.8 mM PEGEEM in distilled water at 95 °C. Within seconds of $HAuCl_4$ addition, the colorless reaction solution immediately turned into a brick red colored dispersion. This color change indicates a fast reduction of Au^{III} to Au^0 and formation of Au nanostructures [20]. Stirring for 15 min and subsequent centrifugation steps produce desired PEG-AuNPs.

Fig. 1a shows a scanning electron microscopy (SEM) image that a large number of Au nanoparticles display a round profile. The transmission electron microscopy (TEM) image in Fig. 1b and c indicates that the average size of the nanoparticles were found to be 21.3 ± 2.2 nm with a monodisperse size distribution of 91%. The elemental composition of the Au nanocrystals shown in the SEM image (Fig. 1a) was determined by energy-dispersive X-ray (EDX)
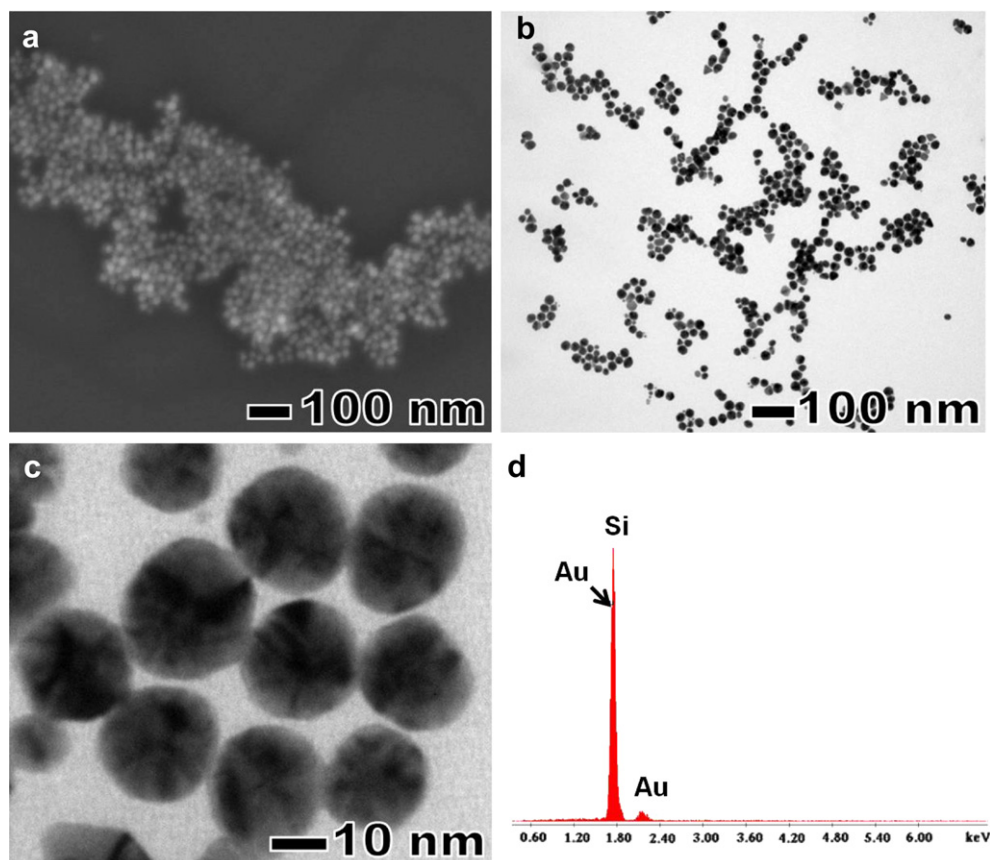
Fig. 1. (a) SEM, (b, c) TEM, and (d) EDX images of multiply-twinned Au nanoparticles synthesized in the presence of 0.057 mM $HAuCl_4$ and 51.8 mM PEGEEM (with a molar ratio of 1:900).

spectroscopy. Using EDX spectrum (Fig. 1d), the nanocrystals were shown to be composed of predominantly Au ($\sim$1.7 and $\sim$2.1 keV) along with silicon atom, a common element on a representative SEM substrate [48].

In order to understand the formation of the Au nanostructures, samples from major events (i.e. color change and growth) were analyzed. Within the first 10 s of the reaction, small Au nanospheres with a diameter ranging from 5 to 10 nm were formed which were exhibited a strong LSPR peak at 533 nm (Fig. 2). As the reaction progressed for another 8 min, larger Au nanocrystals with a diameter of nearly 21 nm were formed with a spectroscopic evidence of a red shift due to an LSPR peak (from 533 to 548 nm) and an increase in the peak intensity. Further extention of reaction time to 15 min caused no significant change in nanoparticle size, shape, or LSPR peak.

To discover the factors that dominate the formation of monodisperse Au nanocrystals, different control experiments were performed by changing the amount of the Au precursor ($HAuCl_4$). Fig. 3 shows TEM images of different Au nanostructures that are formed by varying the concentration of $HAuCl_4$ while keeping the ratio of $HAuCl_4$:PEGEEM constant (1:900, as in the original formulation). This variation resulted the loss of control in particle size and shape. When the concentration of $HAuCl_4$ was decreased to 0.046 mM, polydisperse Au nanocrystals having the average size found to be 22.1 $\pm$ 3.1 nm were obtained as shown in Fig. 3a and b. In comparison, when the concentration of $HAuCl_4$ was increased to 0.071 mM, irregular shapes of Au nanostructures featuring fused nanoparticles were observed (Fig. 3c and d). The average size of these Au nanoparticles was found to be 23.9 $\pm$ 7.3 nm. Therefore,

the concentration of the $HAuCl_4$ in the reaction plays a crucial role in obtaining monodisperse Au nanocrystals.

In order to present the versatile nature of our approach, we tried to apply the reduction process to other noble metals. First, a Pd
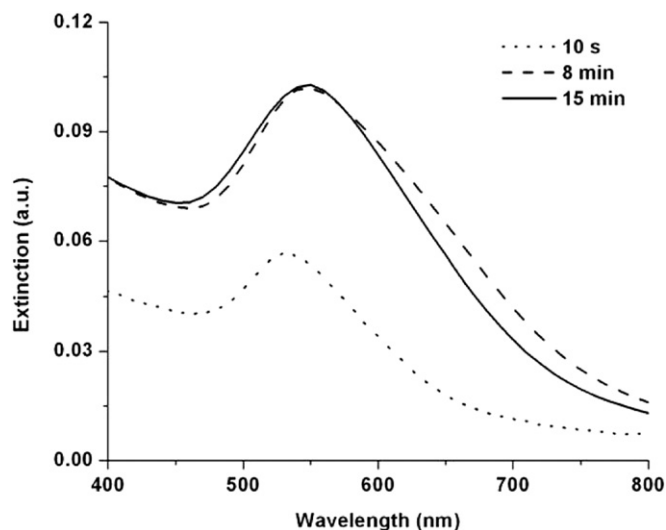

Fig. 2. UV/Vis extinction spectra of the Au samples taken at different reaction times. The dotted, dashed, and solid lines correspond to the samples taken at 10 s, 8 min and 15 min, respectively. The concentrations of $HAuCl_4$ and PEGEEM in the reaction were 0.057 mM and 51.8 mM, respectively.
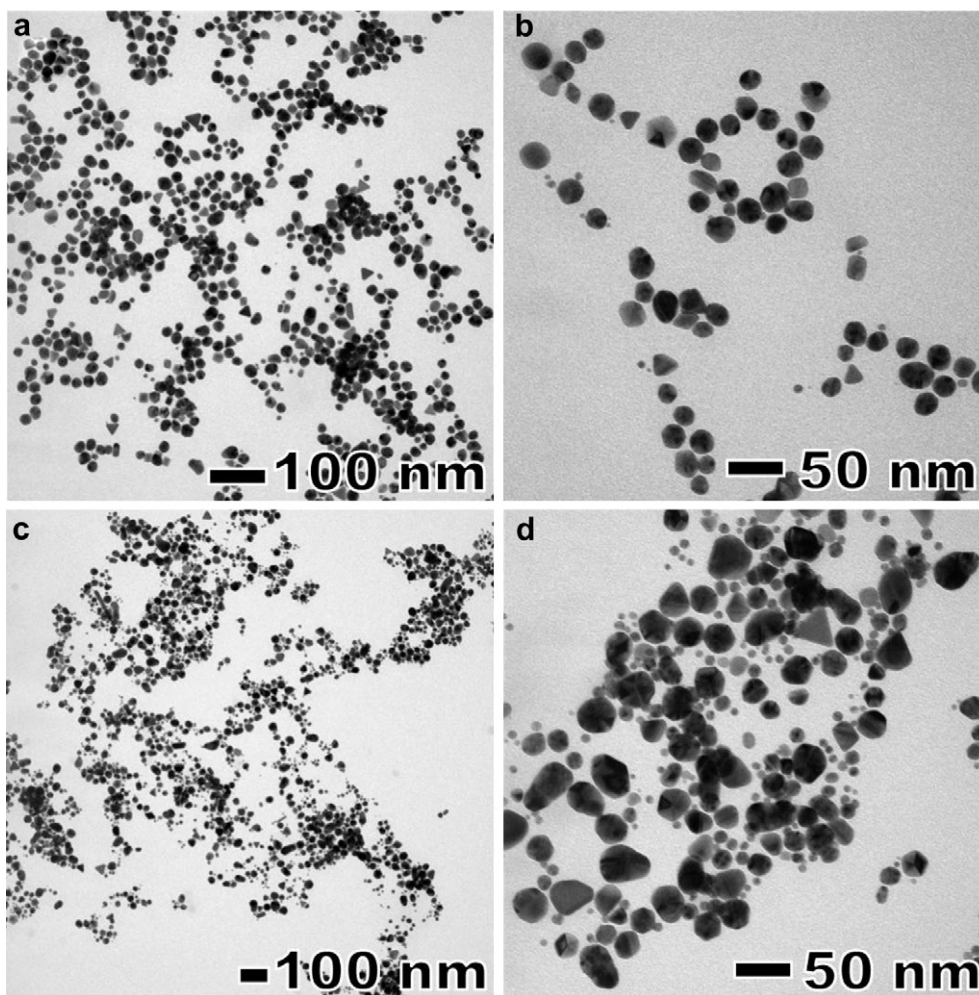
Fig. 3. TEM images of Au samples prepared with the use of (a, b) 0.046 mM and (c, d) 0.071 mM $HAuCl_4$ in the reaction solutions while the molar ratio of $HAuCl_4$ to PEGEEM was kept at 1:900.

precursor (Na_2PdCl_4) was added to PEGEEM reaction solution instead of Au precursor. Fig. 4a and d show the TEM images of the Pd nanoparticle aggregates that resulted from the aqueous reaction of Na_2PdCl_4 and PEGEEM (the same ratio of Au nanocrystal synthesis) at boiling temperature for 15 min. After the addition of Na_2PdCl_4 to pre-heated PEGEEM solution, the color of the reaction solution changed immediately from colorless to gray, and eventually to a brownish gray at the end of 15 min. This color change indicates the reduction of Pd^{II} to Pd^0 and the formation of Pd nanostructures [49]. Fig. 4b also shows the tendency of Pd nanoparticles to form larger aggregates.

In case of Ag, Ag nanocrystals with an average size of 35 nm were collected by mixing $AgNO_3$ and PEGEEM aqueous solutions (the same ratio of Au nanocrystal synthesis) at boiling temperature for 15 min. The color of the reaction solution changed from colorless to light gray in the first few minutes indicating the reduction of Ag^I to its neutral form [50]. The TEM images (Fig. 4c and d) show that the as-prepared Ag nanocrystals are polydisperse and an average diameter of 35 nm.

In a parallel experiment, a structurally similar (featuring 2-methyl substitution on vinyl functionality) but simpler monomer, methyl methacrylate (MMA) was employed as the reductant and stabilizer instead of PEGEEM. MMA showed similar reduction affinities, however, the Au nanostructures resulting from this monomer exhibited significantly different shape and size characteristics (Fig. 5).

The color of the MMA reaction turned to greenish blue color after 15 min as a proof for the formation of Au nanostructures. Several different shapes involving triangular nanoplates, nanokites (a planar head with a quasi-triangular or hexagonal profile) and nanotadpoles were observed (Fig. 5a). A close-up on a complete triangular nanoplate (around 240 nm in size) is shown in Fig. 5b.

We suspect that the reduction of $HAuCl_4$ with PEGEEM follows a similar mechanism reported earlier [52]. In that report that the Au^{III} ion was reduced via alcohol intermediates resulted from the reaction of vinyl groups with water molecules. In this study, it is anticipated that the nucleophilic addition of water molecules to the methyl methacrylate functionality will give two possible alcohol intermediates which are; i) a primary alcohol from terminal methylene ($=CH_2$) part of double bond, and ii) a tertiary alcohol from methyl substituted part of the double bond (Scheme 1). In order to reduce Au^{III} ions to Au, these alcohol intermediates should be able to get oxidized. Since tertiary alcohols cannot oxidize further, the primary alcohol remains as the only choice for a reactive intermediate. Therefore, we believe that this primary alcohol intermediate (**1**) should be responsible for the redox reaction that generates Au nanocrystals from Au^I by reducing to its neutral form (Au^0) resulting an acid by-product (**2**).

Non-specific bovine serum albumin (BSA) adsorption studies were carried out at isoelectric point of the model protein in order to
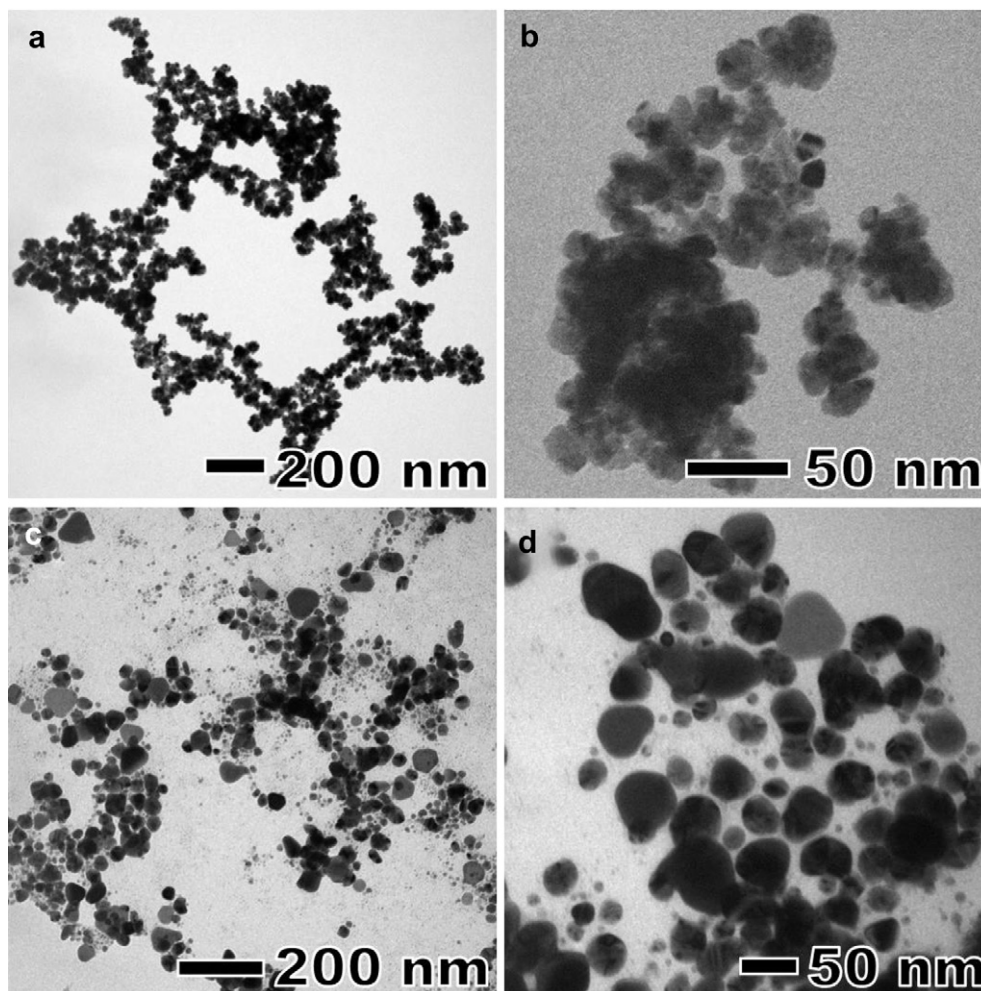
Fig. 4. TEM images of (a, b) Pd and (c, d) Ag samples prepared by using 0.057 mM $AgNO_3$ and 0.172 mM Na_2PdCl_4 as precursors in the reaction, respectively. The molar ratio of the Ag and Pd precursors to PEGEEM was set to 1: 300 and 1:900, respectively. Both reactions were conducted at 95 °C for 15 min.

demonstrate the antifouling property of PEG-AuNPs. Citrate-stabilized Au nanoparticles with similar sizes were prepared to compare protein adsorption. Fig. 6 presents the equilibrium BSA adsorption capacities of these Au nanoparticle formulations at pH 5.0. The pH value was chosen due to the isoelectric point of BSA (pI = 5.0) since maximum adsorption values of protein molecules are usually achieved at their isoelectric points [53–55]. BSA is known to bind to the citrate-stabilized Au nanoparticles with an
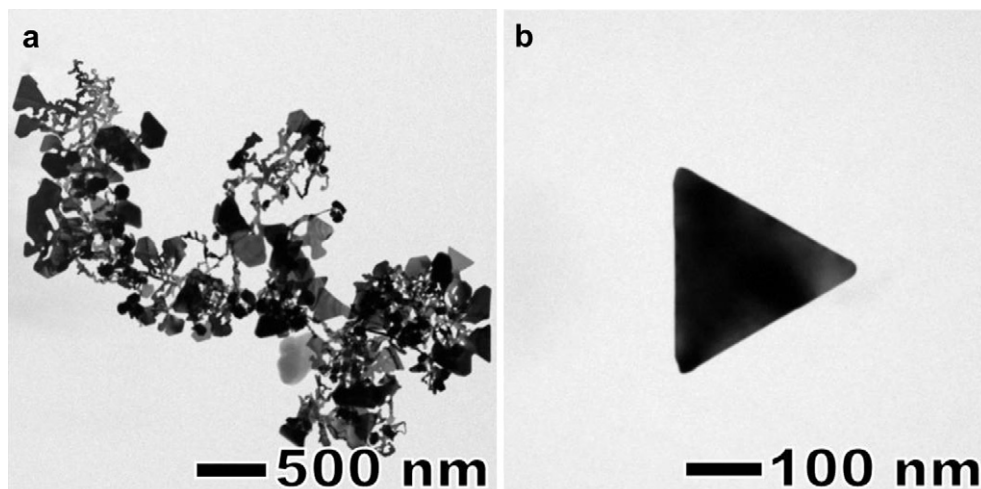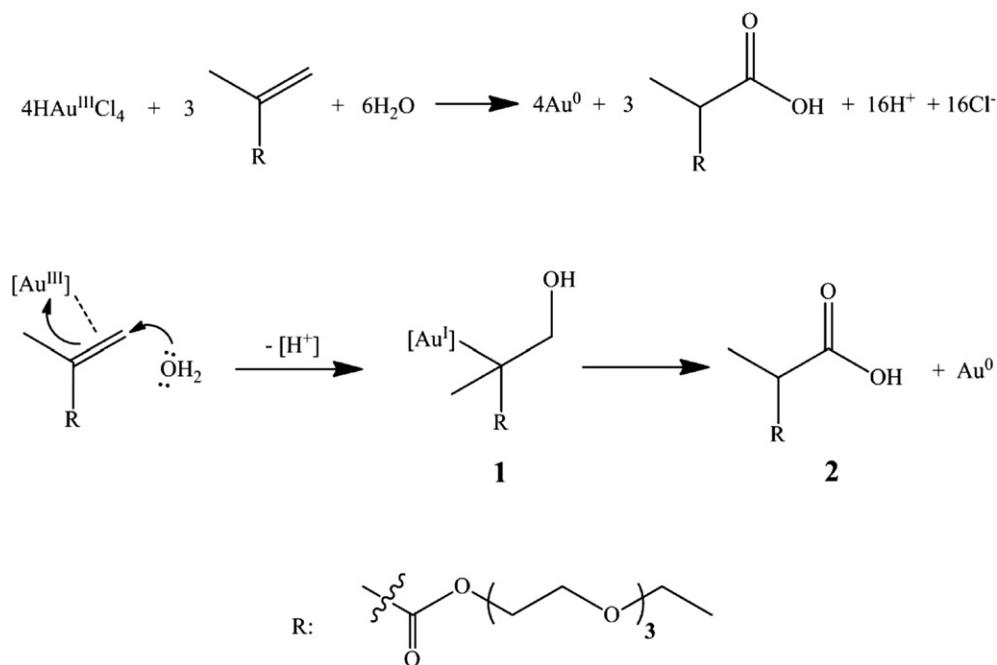

Fig. 5. TEM images of samples prepared with the use of aqueous 0.173 mm $HAuCl_4$ with 156 mM methyl methacrylate solutions. The reactions were conducted at 95 °C for 15 min.

Scheme 1. Proposed mechanism of Au reduction with PEGEEM.

electrostatic binding mechanism as we obtained the same effect shown in Fig. 6 [56–58]. In contrast, PEGEEM-stabilized Au nanoparticles showed no significant non-specific BSA adsorption which could be explained by the steric repulsion effect. The formation of a dynamic molecular cloud by the flexible and electrically neutral PEG species over the nanoparticle surface creates a repulsive effect which thermodynamically inhibits the adsorption of surrounding proteins to PEG-covered surfaces [59]. Our results are also consistent with the literature protein adsorption studies of PEG-coated Au surfaces [60,61].
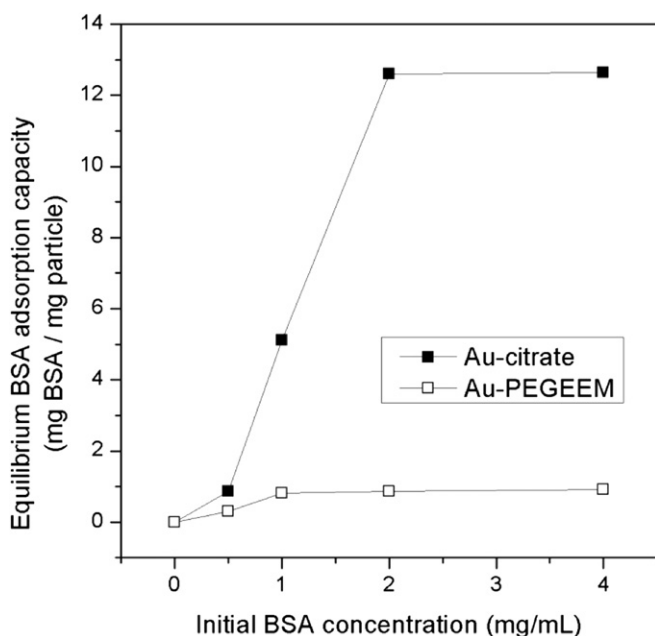

Fig. 6. The variation of equilibrium BSA adsorption capacity with the initial BSA concentration for citrate and PEGEEM-stabilized gold nanoparticles at pH value 5.0.

4. Conclusions

In conclusion, a facile aqueous protocol has been successfully developed for the preparation of PEGylated noble-metal nanoparticles by using PEGEEM. In a typical synthesis, an aqueous metal precursor solution was added to a hot PEGEEM solution for 15 min where PEGEEM served as both an effective reductant and stabilizer. Monodisperse Au nanoparticles were achieved in high yields. The concentration of $HAuCl_4$ in the synthesis was found to play a key role in the formation of monodisperse PEG-AuNPs. When lower or higher concentration of $HAuCl_4$ was used, polydisperse and irregular shapes of Au nanoparticles were obtained. Another chemical reagent bearing similar organic functional groups, methyl methacrylate, was also found effective in the reduction of Au precursor, although unable to control the size and shape of the nanoparticles. The reduction mechanism of Au^{III} ions would have to involve primary alcohol intermediates (the only reductant) which are produced by the nucleophilic addition of water to methacrylic double bond. Pd and Ag precursors resulted polydisperse multiply-twinned Ag nanocrystals and aggregated Pd nanoparticles when added to hot aqueous PEGEEM solution. Furthermore, the PEG-AuNPs demonstrated an excellent blockage of the BSA adsorption (no significant non-specific adsorption) when compared to citrate-coated Au nanoparticles.

References

[1] S. Ferraris, S. Perero, E. Verne, E. Battistella, L. Rimondini, M. Ferraris, Mater. Chem. Phys. 121 (2010) 349–353.

[2] L. Zhou, C. Gao, X. Hu, W. Xu, Chem. Mater. 23 (2011) 1461–1470.
[3] M.S. Yavuz, G.C. Jensen, D.P. Penaloza, T.A.P. Seery, S.A. Pendergraph, J.F. Rusling, G.A. Sotzing, Langmuir 25 (2009) 13120–13124.
[4] G.A. DeVries, M. Brunnbauer, Y. Hu, A.M. Jackson, B. Long, B.T. Neltner, O. Uzun, B.H. Wunsch, F. Stellacci, Science 315 (2007) 358–361.
[5] J.A. Jamison, E.L. Bryant, S.B. Kadali, M.S. Wong, V.L. Colvin, K. Matthews, M.K. Calabretta, J. Nanopart. Res. 13 (2010) 625–636.
[6] K.C.L. Black, Z. Liu, P.B. Messersmith, Chem. Mater. 23 (2011) 1130–1135.
[7] C.M. Niemeyer, Angew. Chem. Int. Ed. 40 (2001) 4128–4158.
[8] S.R. Sershen, S.L. Westcott, N.J. Halas, J.L. West, J. Biomed. Mater. Res. 51 (2000) 293–298.
[9] M.S. Yavuz, Y. Cheng, J. Chen, C.M. Cobley, Q. Zhang, M. Rycenga, J. Xie, C. Kim, K.H. Song, A.G. Schwartz, L.V. Wang, Y. Xia, Nat. Mater. 8 (2009) 935–939.
[10] J.J. Storhoff, A.D. Lucas, V. Garimella, Y.P. Bao, U.R. Muller, Nat. Biotechnol. 22 (2004) 883–887.
[11] C.-H. Wang, C.-J. Liu, C.-C. Chien, H.-T. Chen, T.-E. Hua, W.-H. Leng, H.-H. Chen, I.M. Kempson, Y. Hwu, M. Hsiao, T.-C. Lai, J.L. Wang, C.-S. Yang, H.-M. Lin, Y.-J. Chen, G. Margaritondo, Mater. Chem. Phys. 126 (2011) 352–356.
[12] T.A. Taton, C.A. Mirkin, R.L. Letsinger, Science 289 (2000) 1757–1760.
[13] I.H. El-Sayed, X.H. Huang, M.A. El-Sayed, Nano Lett. 5 (2005) 829–834.
[14] J. Chen, D. Wang, J. Xi, L. Au, A.R. Siekkinen, A. Warsen, Z.-Y. Li, H. Zhang, Y. Xia, X. Li, Nano Lett. 7 (2007) 1318–1322.
[15] S. Lal, S.E. Clare, N. Halas, J. Acc. Chem. Res. 41 (2008) 1842–1851.
[16] V. Mani, B.V. Chikkaveeraiah, V. Patel, J.S. Gutkind, J.F. Rusling, ACS Nano 3 (2009) 585–594.
[17] M. Faraday, Philos. Trans. R. Soc. 147 (1857) 145–181.
[18] M.C. Daniel, D. Astruc, Chem. Rev. 104 (2004) 293–346.
[19] J. Turkevich, P.C. Stevenson, J. Hillier, Discuss. Faraday Soc. 11 (1951) 55–75.
[20] M. Brust, M. Walker, D. Bethell, D.J. Schiffrin, R. Whyman, J. Chem. Soc. Chem. Commun. (1994) 801–802.
[21] T. Mishra, R.K. Sahu, S.-H. Lim, L.G. Salamanca-Riba, S. Bhattacharjee, Mater. Chem. Phys. 123 (2010) 540–545.
[22] H. Hiramatsu, F.E. Osterloh, Chem. Mater. 16 (2004) 2509–2511.
[23] C. Subramaniam, R.T. Tom, T. Pradeep, J. Nanopart. Res. 7 (2005) 209–217.
[24] M. Aslam, L. Fu, M. Su, K. Vijayamohanan, V.P. Dravid, J. Mater. Chem. 14 (2004) 1795–1797.
[25] N. Zheng, J. Fan, G.D. Stucky, J. Am. Chem. Soc. 128 (2006) 6550–6551.
[26] P. Calandra, C. Giordano, A. Longo, V.T. Liveri, Mater. Chem. Phys. 98 (2006) 494–499.
[27] E. Hoppe, M. Lazzari, I. Pardinas-Blanco, M.A. Lopez-Quintela, Langmuir 22 (2006) 7027–7034.
[28] X. Shi, K. Sun, J.R. Baker, J. Phys. Chem. C. 112 (2008) 8251–8258.
[29] G. Jiang, L. Wang, T. Chen, H. Yu, C. Chen, Mater. Chem. Phys. 98 (2006) 76–82.
[30] M. Shen, K. Sun, X. Shi, Curr. Nanosci. 6 (2010) 307–314.
[31] G. Zhanga, Z. Yanga, W. Lua, R. Zhanga, Q. Huanga, M. Tiana, L. Lib, D. Liangc, C. Lia, Biomaterials 30 (2009) 1928–1936.
[32] H. Furusho, K. Kitano, S. Hamaguchi, Y. Nagasaki, Chem. Mater. 21 (2009) 3526–3535.
[33] B. Ballou, B.C. Lagerholm, L.A. Ernst, M.P. Bruchez, A.S. Waggoner, Bioconjug. Chem. 15 (2004) 79–86.
[34] C. Kirchner, T. Liedl, S. Kudera, T. Pellegrino, M.A. Javier, H.E. Gaub, S. Stlzle, N. Fertig, W. Parak, J. Nano Lett. 5 (2005) 331–338.
[35] H. Otsuka, Y. Nagasaki, K. Kataoka, Adv. Drug Deliv. Rev. 55 (2003) 403–419.
[36] J.P. Bearinger, S. Terrettaz, R. Michel, N. Tirelli, H. Vogel, M. Textor, J.A. Hubbell, Nat. Mater. 2 (2003) 259–264.
[37] G.F. Paciotti, L. Myer, D. Weinreich, D. Goia, N. Pavel, R.E. McLaughlin, L. Tamarkin, Drug Deliv. 11 (2004) 169–183.
[38] W.D. James, L.R. Hirsche, J.L. West, P.D. O'Neal, J.D. Payne, J. Radioanal. Nucl. Chem. 271 (2007) 455–459.
[39] G. Prencipe, S.M. Tabakman, K. Welsher, Z. Liu, A.P. Goodwin, L. Zhang, J. Henry, H. Dai, J. Am. Chem. Soc. 131 (2009) 4783–4787.
[40] C. Fernandez-Lopez, C. Mateo-Mateo, R.A. Alvarez-Puebla, J. Perez-Juste, I. Pastoriza-Santos, L.M. Liz-Marzan, Langmuir 25 (2009) 13894–13899.
[41] W.P. Wuelfing, S.M. Gross, D.T. Miles, R.W. Murray, J. Am. Chem. Soc. 120 (1998) 12696–12697.
[42] T. Niidome, M. Yamagata, Y. Okamoto, Y. Akiyama, H. Takahashi, T. Kawano, K. Katayama, Y. Niidome, J. Control. Release 114 (2006) 343–347.
[43] T. Ishii, H. Otsuka, K. Kataoka, Y. Nagasaki, Langmuir 20 (2004) 561–564.
[44] C. Kojima, Y. Umeda, A. Harada, K. Kono, Colloids Surf. B. 81 (2010) 648–651.
[45] A.T. Naeini, M. Adeli, M. Vossoughi, Eur. Poly. J. 46 (2010) 165–170.
[46] C. Peng, L. Zheng, Q. Chen, M. Shen, R. Guo, H. Wang, X. Cao, G. Zhang, X. Shi, Biomaterials 33 (2012) 1107–1119.
[47] P. Pengo, S. Polizzi, M. Battagliarin, L. Pasquato, P. Scrimin, J. Mater. Chem. 13 (2003) 2471–2478.
[48] Y. Lu, H. Xiong, X. Jiang, Y. Xia, M. Prentiss, G.M. Whitesides, J. Am. Chem. Soc. 125 (2003) 12724–12725.
[49] E. Formo, M.S. Yavuz, E.P. Lee, L. Lane, Y. Xia, J. Mater. Chem. 19 (2009) 3878–3882.
[50] V.N. Richards, N.P. Rath, W.E. Buhro, Chem. Mater. 22 (2010) 3556–3567.
[51] E.C. Cho, J. Xie, P.A. Wurm, Y. Xia, Nano Lett. 9 (2009) 1080–1084.
[52] M.S. Yavuz, W. Li, Y. Xia, J. Chem. Eur. J. 15 (2009) 13181–13187.
[53] X.F. Yuan, D. Fabregat, K. Yoshimoto, Y. Nagasaki, Anal. Chem. 81 (2009) 10097–10105.
[54] T. Camli, M. Tuncel, S. Senel, A. Tuncel, J. Appl. Polym. Sci. 84 (2002) 414–429.
[55] A. Denizli, G. Kokturk, H. Yavuz, E. Piskin, J. Appl. Polym. Sci. 74 (1999) 2803–2810.
[56] S.H. Brewer, W.R. Glomm, M.C. Johnson, M.K. Knag, S. Franzen, Langmuir 21 (2005) 9303–9307.
[57] W.R. Glomm, O. Halskau, A.D. Hanneseth, S. Volden, J. Phys. Chem. B 111 (2007) 14329–14345.
[58] S. Pihlasolo, J. Kirjavainen, P. Hanninen, H. Harma, Anal. Chem. 81 (2009) 4995–5000.
[59] A.S. Zahr, C.A. Davis, M.V. Pishko, Langmuir 22 (2006) 8178–8185.
[60] A. Rastogi, S. Nad, M. Tanaka, N. Da Mota, M. Tague, B.A. Baird, H.D. Abruna, C.K. Ober, Biomacromolecules 10 (2009) 2750–2758.
[61] K.L. Prime, G.M. Whitesides, J. Am. Chem. Soc. 115 (1993) 10714–10721.